Seasonal drivers of understorey temperature buffering in temperate deciduous forests across Europe

Florian Zellweger, David Coomes, Jonathan Roger Michel Henri Lenoir, Leen Depauw, Sybryn Maes, Monika Wulf, Keith Kirby, Jörg Brunet, Martin Kopecký, František Máliš, et al.

Seasonal drivers of understorey temperature buffering in temperate deciduous forests across Europe

Florian Zellweger, David Coomes, Jonathan Lenoir, Leen Depauw, Sybryn Maes, Monika Wulf, Keith Kirby, Jörg Brunet, Martin Kopecký, František Máliš, et al.

Seasonal drivers of understorey temperature buffering in temperate deciduous forests across Europe

Running Title: Drivers of understorey temperature buffering

Florian Zellweger[1,2], *David Coomes*[1], *Jonathan Lenoir*[3], *Leen Depauw*[4], *Sybryn L. Maes*[4] *Monika Wul*[5], *Keith Kirby*[6], *Jörg Brunet*[7], *Martin Kopecky*[8,9], *Frantisek Malis*[10], *Wolfgang Schmidt*[11], *Steffi Heinrichs*[11], *Jan den Ouden*[12], *Bogdan Jaroszewicz*[13], *Gauthier Buyse*[4], *Fabien Spicher*[3], *Kris Verheyen*[4], *Pieter De Frenne*[4]

[1] Forest Ecology and Conservation Group, Department of Plant Sciences, University of Cambridge, Cambridge, UK
[2] Swiss Federal Institute for Forest, Snow and Landscape Research WSL, Zürcherstrasse 111, 8903 Birmensdorf, Switzerland
[3] UR "Ecologie et dynamique des systems anthropisés" (EDYSAN, UMR 7058 CNRS-UPJV), Université de Picardie Jules Verne, Amiens Cedex 1, France
[4] Forest & Nature Lab, Department of Environment, Ghent University, Melle-Gontrode, Belgium
[5] Leibniz-ZALF e.V. Müncheberg, Müncheberg, Germany
[6] Department of Plant Sciences, University of Oxford, Oxford, UK
[7] Southern Swedish Forest Research Centre, Swedish University of Agricultural Sciences, Alnarp, Sweden
[8] Institute of Botany, Czech Academy of Sciences, Průhonice, Czech Republic
[9] Faculty of Forestry and Wood Sciences, Czech University of Life Sciences Prague, Czech Republic
[10] Faculty of Forestry, Technical University in Zvolen, Zvolen, Slovakia
[11] Department Silviculture and Forest Ecology of the Temperate Zones, University of Göttingen, Göttingen, Germany
[12] Forest Ecology and Forest Management Group, Wageningen University, Wageningen, The Netherlands
[13] Białowieża Geobotanical Station, Faculty of Biology, University of Warsaw, Białowieża, Poland

Corresponding author: F. Zellweger (fz255@cam.ac.uk) and D. Coomes (dac18@cam.ac.uk)

Abstract

Aim: Forest understory microclimates are often buffered against extreme heat or cold, with important implications for the organisms living in these environments. We quantified seasonal effects of understory microclimate predictors describing canopy structure, canopy composition and topography (i.e. local factors), as well as forest patch size and distance to coast (i.e. landscape factors).

Location: Temperate forests in Europe

Time period: 2017-2018

Major taxa studied: Woody plants

Methods: We combined data from a microclimate sensor network with weather station records to calculate the difference – or offset – between temperatures measured inside and outside forests. We used regression analysis to study the effects of local and landscape factors on the seasonal offset of minimum, mean and maximum temperatures.

Results: Maximum temperature during summer was on average cooler by 2.1 °C and minimum temperature during winter and spring were 0.4 °C and 0.9 °C warmer inside than outside forests. The local canopy cover was a strong non-linear driver of the maximum temperature offset during summer, and we found increased cooling beneath tree species that cast the deepest shade. Seasonal offsets of minimum temperature were mainly regulated by landscape and topographic features, such as the distance to coast and topographic position.

Main conclusions: Forest organisms experience less severe temperature extremes than suggested by currently available macroclimate data, so climate-species relationships and species' responses to anthropogenic global warming cannot be modelled accurately in forests using macroclimate data alone. Changes in canopy cover and composition will strongly modulate warming of maximum temperatures in forest understories, with important implications for understanding responses of forest biodiversity and functioning to the

combined threats of land-use change and climate change. Our predictive models are generally applicable across lowland temperate deciduous forests, providing ecologically important microclimate data for forest understories.

Keywords: Canopy Density, Climate Change, Forest Structure and Composition, Global Warming, Macroclimate, Microclimate, Temperature Buffering, Understorey

Introduction

The global network of standardised weather stations deliberately excludes forest microclimate, focussing instead on measuring synoptic, free-air conditions representing the macroclimate (De Frenne & Verheyen, 2016). Such weather stations are dictating the global climate data layers available for ecological research (e.g., CHELSA (Karger *et al.*, 2017) and Worldclim (Fick & Hijmans, 2017)), despite the fact that such data do not well represent the climatic conditions many forest organisms experience (Potter *et al.*, 2013; Bramer *et al.*, 2018). We thus know relatively little about forest microclimate gradients across large spatial scales and over time. This is a major impediment for global change biology because forests cover almost one third of the land surface on Earth and harbour about two thirds of all terrestrial biodiversity (MEA, 2005; FAO, 2010).

Variation in forest structure, composition and topographic position leads to highly heterogeneous microclimate across space and time, with important consequences for the growth, survival and reproductive success of forest organisms and for forest functioning (Bazzaz & Wayne, 1994). The significance of microclimate has been acknowledged by ecologists and foresters for a long time and microclimate is increasingly recognised as an important moderator of biotic responses to anthropogenic climate change (Uvarov, 1931; Geiger *et al.*, 2003; Lenoir *et al.*, 2017). For example, canopy structure and the associated microclimatic conditions strongly mediate forest species responses to climate warming (De Frenne *et al.*, 2013; Scheffers *et al.*, 2014). Locally experienced warming rates due to anthropogenic climate and land-use change are strongly modified by changes in canopy structure, e.g., by changes in canopy cover. Quantifying the variability of forest temperature in space and over time will thus be key to addressing the responses of forest organisms to climate and land use change (Lenoir *et al.*, 2017).

One potential route to derive forest microclimate dynamics is to infer them from climate data available from weather stations. Advanced modelling approaches, such as the mechanistic downscaling of microclimate from interpolated weather station data, make it increasingly feasible to approximate microclimate across space and over time (Bramer *et al.*, 2018; Zellweger *et al.*, 2019). However, attempts to model forest microclimates are rare and often lack appropriate data for model calibration and validation (Kearney & Porter, 2017; Maclean *et al.*, 2018). We need empirical, generalizable data at large spatial scales to further our understanding of the drivers of the differences between climatic measurements made inside forests and those made by nearby weather stations outside forests (Jucker *et al.*, 2018). These could then be combined with the wealth of data describing forest structure and composition (e.g., collected within national forest inventories) to pave the way to translating past, present and projected macroclimate data into better representations of the climate conditions that forest organisms actually experience (Bramer *et al.*, 2018). Yet, quantitative assessments of forest microclimates at broad spatial scales and over sufficient timespans to detect seasonal effect sizes of key drivers of microclimate are still scarce (Greiser *et al.*, 2018).

Across all major biomes understory temperatures are offset to free-air conditions by one to four degrees or more, resulting in buffered, i.e. less extreme, temperature regimes below tree canopies (De Frenne *et al.*, 2019). Maximum daytime temperatures in woodland understories are cooled by tree canopies because they reduce transmission of shortwave solar radiation to the understorey and cool the air by transpiration (Davis *et al.*, 2019). Tree canopies reduce radiative heat loss and emit some of the energy absorbed during the day to the understorey, thereby causing warmer daily minimum temperatures in the understorey compared to free-air conditions (Geiger *et al.*, 2003). Although less often studied, canopy composition may also affect the microclimate because the quality and quantity of light transmitted by canopy foliage varies among tree species, leading to subtle species-specific

119 effects on the light conditions and associated microclimates (Renaud & Rebetez, 2009).
120 However, despite a growing number of studies showing that canopy cover, basal area and/or
121 canopy height are major determinants of understorey temperatures (Chen *et al.*, 1999; von Arx
122 *et al.*, 2013; Greiser *et al.*, 2018; Jucker *et al.*, 2018), we still lack a general model of the form
123 of the relationship at continental scales.

124 Differences between macro- and microclimate, i.e. temperature offsets, result from
125 processes operating at multiple scales and their influence may change over the course of the
126 seasons. Topographic position and slope exposure have strong influences on radiation regimes
127 and microclimatic gradients; for example, cold air drainage lowers daily minimum
128 temperatures in areas where cold air flows and settles (Daly *et al.*, 2010), resulting in increased
129 temperature offsets (Lenoir *et al.*, 2017). Such effects represent the influence of regional terrain
130 features on local climate dynamics and are expected to be largely independent from effects
131 brought about by local canopy characteristics. Wind mixes air and reduces the differences
132 between the macro- and microclimate. The levels of air mixing and lateral transfer of humidity
133 and heat by wind generally decrease with increasing distance from the coast, from the edge of
134 forest patches, or with increasing forest structural complexity, leading to increased temperature
135 offsets (Kovács *et al.*, 2017; Bramer *et al.*, 2018). At continental and global scales, the
136 magnitude of the temperature offset varies considerably across biomes and forest types,
137 suggesting that the macroclimate may explain some of the variation in microclimatic buffering
138 (De Frenne *et al.*, 2019). To put the influence of local drivers of microclimate into perspective,
139 it will thus be important to study potential drivers at multiple spatial and temporal scales, and
140 to make systematic measurements at continental scales.

141 Here we quantify the differences between air temperatures measured in the understorey
142 and nearby weather stations in sites spanning much of the temperate deciduous forest biome of
143 Europe. We analysed the seasonal variation in these temperature differences and compared the

relative importance of (1) local canopy structure and composition *versus* (2) variables describing the landscape structure and the topography to explain this variability.

Materials and Methods

Sampling design and study sites

We compiled data from ten regions spanning an East – West gradient of c. 1700 km and a North – South gradient of c. 800 km across a major part of the European temperate deciduous forest biome (Figure 1). In each region, we selected ten plots representing a regional gradient of canopy cover. This resulted in 100 plots varying in total canopy cover (cumulative sum across all species and vertical layers) from as little as 41 % up to 213 %. The dominant tree species in terms of cover (with the number of plots in which they occur) were *Fagus sylvatica* (47), *Carpinus betulus* (44), *Fraxinus excelsior* (39), *Quercus robur* (34) *and Quercus petraea* (30). The mean annual temperature and precipitation during the time period 1979 - 2013 ranged from 7.3 to 11.0 °C and 468 to 1000 mm across the studied regions, respectively (Karger *et al.*, 2017).

Measurement of temperature and dependent variables

In each plot we recorded air temperature every hour from 22 February 2017 to 21 February 2018, using Lascar EasyLog EL-USB-1 temperature sensors with an accuracy of ± 0.5 °C. The sensors were attached to a tree trunk with DBH > 25 cm at 1 m above ground, which marked the centre of the plot (Figure 1c). To exclude potential bias due to direct sunlight, we placed the loggers in 18 cm long white plastic radiation shields which we attached at the north side of the tree trunk (see Supporting Information Figure S1; in Appendix S1). We aggregated the hourly temperature data to three daily temperature statistics: minimum daily (Tmin), mean daily (Tmean) and maximum (Tmax) daily temperature. All daily time series were plotted, visually checked for obvious outliers and compared to all other times series within the respective region, including the respective temperature time series that we obtained from the

169 closest weather station. This allowed us to verify and exclude sampling periods that were
170 potentially biased due to temporary device malfunction or misplacement (e.g. logger found on
171 the ground due to disturbance from wild boar, bear, deer, etc.). As a result, our sample sizes
172 for spring, summer, autumn and winter were 92, 96, 95, and 98 plots, respectively.

173 We defined temperature offset values as the difference between the daily temperature
174 statistics (Tmin, Tmean, Tmax) recorded inside the forest and the respective temperature
175 statistic recorded by the closest official weather station representing free-air conditions outside
176 forests. The temperature offsets for Tmin, Tmean and Tmax are our dependent variables.
177 Negative offsets thus indicate cooler, and positive offset values warmer temperatures inside
178 *versus* outside forests. We focus on temperature offsets rather than absolute values to facilitate
179 among-region comparisons across Europe, because macroclimate-microclimate temperature
180 differences are most relevant for species' responses to climate change, and because temporal
181 temperature changes due to anthropogenic climate change are also expressed against a baseline.

182 To account for temperature differences due to differences in elevation between the
183 locations of the sensor and the weather station, we applied a constant lapse rate of 0.5 °C per
184 100 m for Tmin and Tmean, and a seasonal lapse rate for Tmax: 0.5° C in winter, 0.7° C in
185 spring and summer, and 0.6° C in autumn. The choice of lapse rates were guided by empirical
186 evidence from several regions in Europe (Rolland, 2003; Kollas *et al.*, 2014). Our study focus
187 lies on lowland forests and the differences in elevation between the plots and weather stations
188 ranged between 1 and 284 m, with a median of 35 m (Appendix S2). Although lapse rates may
189 vary between sites, seasons and temperature statistics (Tmin, Tmean, Tmax), such unaccounted
190 variation in lapse rates would result in only minor differences in offset values, not affecting
191 our main findings and conclusions. This is empirically supported by a lack of residual
192 correlation of our models and data with the elevational differences between locations of the
193 sensor and the weather station (Appendix S2).

We aggregated daily temperature offsets to calculate monthly means, as well as means across the meteorological seasons, i.e., spring (March, April, May), summer (June, July, August), autumn (September, October, November) and winter (December, January, February). Absolute minimum temperatures can be a crucial factor limiting plant survival, so we calculated the offset value for the absolute daily minimum temperature during winter, as well as during spring (Kollas *et al.*, 2013).

Measurement of explanatory variables

We applied a combination of field-based surveys and published spatial data to derive two groups of explanatory variables representing (1) local canopy structure and composition *versus* (2) landscape structure and topography (Table 1). Local-scale canopy structure and composition was assessed between 3 July and 15 August 2017, within a circular plot area with a radius of 9 m around the central tree on which the temperature sensor was attached (Figure 1c). The plot dimensions were measured with a vertex hypsometer (Vertex IV), and the location of the interpretation point in each cardinal direction was marked with a pole. The coordinates of the plot centre were recorded using a differential Global Positioning System with an accuracy of *c.* 1 m. In each cardinal direction, we visually estimated canopy cover, by adding up the species-specific vertical covers of all the plant species in the shrub and tree layer. The shrub and tree layers included all trees and shrubs with heights between 1 and 7 m, and above 7 m, respectively. *Canopy cover* per plot was then calculated as the mean of these four estimations. The species-level approach for estimating canopy cover provides a detailed measure of the cumulative sum of cover across all species and vertical layers, allowing values to exceed 100 percent due to overlaps. At the stand level, however, canopy cover estimates are often confined within the range of 0 to 100 percent. We therefore also analysed a transformed version of our canopy cover values by accounting for the overlap and constraining the cumulative cover values below 100 percent (see Appendix S9 for details). *Canopy openness*

was measured by taking the mean of spherical densiometer readings taken in the four subplots. We used a concave spherical densiometer, which displays large parts of the sky hemisphere, thus enabling us to take an angular view for estimating the fraction of sky hemisphere not covered by the canopy (Baudry *et al.*, 2014). It is important to note that our estimates of canopy cover and canopy openness represent one snapshot in time, neglecting temporal variation in leaf area and associated effects on microclimates. *Basal area* was estimated based on the diameter at breast height (DBH) of all trees within the plot with a minimal DBH of 7.5 cm, as measured with callipers. The total sum of projected *crown area (CA)* for all individual tree species was estimated based on the allometric relationship between CA and DBH (Jucker *et al.*, 2016) (see Appendix S3 for details). We considered CA as an additional variable because its link to microclimate is more mechanistic compared to DBH. The *height of the tree* on which the temperature logger was attached was measured by the mean of two measurements from opposing directions using the vertex hypsometer (Vertex IV). The *shade casting ability* (SCA) describes the ability of each tree species to cast a specific level of shade, ranging between 1 (very low shade casting ability, e.g. *Betula* spp.*)* and 5 (very high shade casting ability, e.g. *Fagus sylvatica*) (Verheyen *et al.*, 2012). We calculated a weighted SCA per plot by using the species-specific canopy cover estimates as weights. This allowed us to test whether canopies made out of tree species with higher SCA scores have a stronger offsetting capacity than those with low SCA scores.

Landscape and topographic characteristics were derived from satellite-based global tree cover data with a spatial resolution of *c*. 30 m (Hansen *et al.*, 2013) and a pan-European digital elevation model (DEM) with a spatial resolution of 25 m, using Copernicus data and information from the European Union (EU-DEM, 2018). *Forest cover* was assessed within a circular buffer area with a radius of 250 m and measured as the percentage of area covered by a minimum tree cover of 20 % (Hansen *et al.*, 2013). *Distance to forest edge* was calculated by

transforming the forest cover mask into contour lines and extracting the distance from the plot coordinate to the nearest contour line, using the *rasterToContour* and *gDistance* functions in the R packages "raster" (Hijmans, 2017) and "rgeos" (Bivand & Rundel, 2018). Landscape-level forest cover and distance to edge have previously been related to forest microclimates (Latimer & Zuckerberg, 2017; Greiser *et al.*, 2018) and may affect the level of air mixing and the lateral transfer of heat and humidity by wind, thus affecting the temperature offset. *Topographic northness*, *slope*, *elevation* and *topographic position* were all derived from the DEM to represent topographic effects on the offset of understorey temperatures, including variation in solar radiation incidence and cold air drainage, an important process affecting minimum temperatures at night and during winter (Daly *et al.*, 2010; Ashcroft & Gollan, 2013). Topographic northness describes the topographic exposition ranging from completely north exposed to completely south exposed, and was derived as cosine of topographic aspect. Topographic position was calculated as the difference between the elevation of the plot cell and the lowest cell within a circular buffer area with a radius of 500 m (Ashcroft & Gollan, 2013). We further considered the *distance to the nearest coastline* because the temperature offset may increase with increasing distance to coast, due to increased temperature ranges and lower levels of air mixing.

Statistical analysis

To analyze the relative importance of our two groups of predictor variables, i.e., local canopy characteristics *versus* landscape-level metrics, for explaining temperature offsets we used variation partitioning following Borcard *et al.* (1992). First, we performed a principal components analysis (PCA) for each of the variable groups and used the first two axes per group as predictor variables in the subsequent analysis. Thus, the number of predictor variables used per group was the same. Among canopy characteristics, crown area and canopy cover had the highest loadings on the first and second PCA axis, respectively, while the loadings for the

landscape metrics were more variable among predictor variables (Appendix S4). We then fitted linear mixed-effects models (LMMs) with the PCA axes as fixed effects and 'region' as a random intercept term to account for the non-independence among replicates from the same region, using restricted maximum likelihood in the *lmer* function from the lme4-package (Bates *et al.*, 2015). We did not include a random slope term because it resulted in higher AIC values when compared to the models with random intercepts only. We fitted three LMMs: one for each of the two variable groups (local canopy characteristics *versus* landscape-level metrics) and one for the combination of both groups. Based on these three LMMs we finally partitioned the amount of explained variation (marginal R^2) into individual and shared fractions (Borcard *et al.*, 1992).

To report the relationship between each individual predictor variable and each dependent variable (i.e, the offset values for Tmin, Tmean and Tmax) we performed χ2-tests by comparing the univariate LMM including each single predictor (scaled to a mean of 0 and standard deviation of 1) with a respective intercept-only model, both with 'region' as a random intercept term (Zuur *et al.*, 2009). We log-transformed canopy openness and topographic position to better conform to normality. Goodness-of-fit was determined by calculating marginal and conditional R^2 values following (Nakagawa & Schielzeth, 2012) using the *r.squaredGLMM* function in the MuMIn-package (Barton, 2018). The marginal R^2 describes the variation explained by the fixed factors only, whereas the conditional R^2 describes the variation explained by the fixed and random factors together (Nakagawa & Schielzeth, 2012).

We expected that the random intercept term 'region' would capture major gradients in macroclimate in our sampling design (Figure 1), leaving little variation in temperature offset to be explained by macroclimate once regional effects have been accounted for. To test this assumption, we performed an additional variation partitioning exercise with three variables groups, i.e., the two groups representing local canopy characteristics and landscape-level

metrics, and an additional group representing the macroclimate. The variables in the latter group were the long-term (1979 – 2013) mean annual precipitation and temperature (Karger *et al.*, 2017), as well as the daily minimum, maximum and mean temperature statistics from the weather stations for the 1-year period matching with the understorey temperature sensors' data, aggregated over the same time periods as the dependent variables. Following the approach chosen for the two other groups of local canopy characteristics and landscape-level metrics and to ensure that the number of predictor variables used per group was the same, we used the first two axes of a PCA on macroclimate variables as predictor variables in the variation partitioning (Appendix S4).

To test for non-linear relationships between the temperature offset and canopy characteristics, as well as topographic position, we used general additive mixed-effects models (GAMMs) with the *gamm* function in the "mgcv" package (Wood, 2017) and again 'region' was added as random term. To complement the non-linearity check and to identify possible break points or thresholds, we used piecewise regression based on the function *segmented* in the "segmented" package (Muggeo, 2017). To investigate the degree to which the relationships between canopy characteristics and temperature offset are transferable to other regions across the temperate deciduous forest biome, we assessed the model's predictive performance based on a cross-validation procedure with blocked data splitting, accounting for our hierarchical sampling design ('region' as a random effect) (Roberts *et al.*, 2017). To this end, we calibrated ten different models for each of the six canopy variables, i.e. 60 models in total. Each model was calibrated using the data from nine regions, and validated based on the predictions made to the 10th, left-out region. For the sake of parsimony, we combined each canopy variable with only one variable describing landscape structure and topography, i.e. distance to the coast, which had a relatively large influence on the magnitude of the offset value for maximum temperatures (see results). We refrained from analysing the predictive performance of the

landscape structure and topography variables, because our focus here was primarily on the effects of the canopy structure and composition. Canopy variables were relatively unimportant for explaining variation in the offset of Tmin, so we restricted our analysis to Tmax. Predictive performance was assessed based on the R^2-value comparing the predicted vs. the observed values. All analyses were performed in R version 3.5.0 (R Core Team, 2018).

Results

The mean (range) daily maximum air temperature (Tmax) offset during summer was -2.1 °C (-3.7 to 1.4) and mean daily minimum air temperature (Tmin) offset during winter was 0.4 °C (-1.2 to 2.0) (Figure 2). Across all regions and the whole year, the mean offset of Tmax and Tmin was -0.8 °C (-2.3 to 1.6) and 0.9 °C (-0.6 to 2.8), respectively. The offset of daily average temperatures (Tmean) was generally low, with means of -0.5 °C (-1.4 to 0.4) during summer and -0.03 °C (-0.8 to 0.8) during winter.

The offset of temperature extremes varied considerably between the sampled regions and months and seasons, and was most pronounced during summer and least distinctive during winter (Figure 2 and Appendix S5). Interestingly, the offset of Tmax during spring were slightly positive, with a mean of 0.4 °C (-2.4 to 3.0), indicating that spring Tmax inside forests may often be higher, not lower, than outside forests. The average offset of Tmin in spring was also positive, i.e. mean daily minimum temperatures in spring were warmer by 0.9 °C (-1.4 to 3.6) in the understorey than outside forests. The same pattern was found for absolute daily minimum temperature offset during spring and winter, with means of 0.9 °C (-1.7 to 3.2) and 1.5 °C (-1.1 to 5.4), respectively (Appendix S6).

Partitioning the explained variance into independent contributions of local canopy characteristics *versus* landscape and topography metrics, as well as their joint contributions, showed that canopy characteristics were generally more important for explaining the variation in Tmax offsets, while landscape and topography metrics were most important for explaining Tmin offsets (Figure 3). During summer, the independent effect of canopy characteristics on Tmax offset was greatest, with a marginal $R^2 = 0.22$. During winter, landscape and topography metrics independently explained 40 % of the variation (marginal $R^2 = 0.4$) in Tmin offset. The joint contributions between canopy characteristics and landscape and topography metrics were low, suggesting that the groups capture different processes governing forest microclimates.

The total marginal R^2 values for Tmax offset during summer and Tmin offset during winter were both 0.41, and thus considerably higher than the R^2-values for Tmin and Tmax offset during spring and autumn, which ranged between 0.13 and 0.27 (Figure 3). In line with our expectation, including the macroclimate as a third variable group in the variation partitioning revealed relatively small independent effects of macroclimate, except for Tmin in spring (Figure S7).

Analysis of the independent effect of canopy characteristics on the offset of Tmax during summer revealed a negative and non-linear relationship for canopy cover, i.e., the cooling of Tmax in the understorey increased non-linearly with increasing canopy cover (Figure 4). Piecewise regression analysis identified a canopy cover threshold at 89 % (standard error 8.5 %), below which the offsetting capacity of canopy cover rapidly increased when additional vegetation cover was added. The results for the transformed version of canopy cover with values constraint to range between 0 and 100 % suggest a threshold of 75 % (standard error 5.2 %) and a comparably weak non-linearity (Appendix S9). Non-linear relationships were further found for canopy openness and crown area, but not for basal area, which was weakly and negatively related to the offset of Tmax during summer (Figure 4 and Table S8). Contrary to our expectations, the Tmax offset increased with increasing tree height, suggesting a decrease in temperature buffering. However, this relationship was weak and we thus refrain from further interpreting this result.

The shade casting ability (SCA) of the tree species composition was significantly and negatively related to the offset of Tmax, indicating that the buffering capacity increases with increasing SCA (Figure 4). SCA was not correlated with any of the canopy structure metrics tested, suggesting that the canopy composition holds information for explaining the temperature offset that is complementary to canopy structure (Appendix S10).

The topographic position, distance to the coast and elevation were the most important predictors for Tmin offset across the seasons (Table S8). The minimum temperature offsets increased linearly with increasing distance to coast, explaining 39 % of the variation for Tmin during winter and 17 % of the variation for Tmax during summer (Figure 5; Table S8). Elevation and distance to coast were strongly correlated (Pearson's r: 0.84, Figure S10) and thus showed similar patterns. We therefore do not further elaborate on the effects of elevation on the temperature offset. Topographic position was non-linearly related to the offset of Tmin in winter (Figure 5), and was also an important predictor of the offset of the absolute daily minimum temperature in winter and spring (Table S6). Landscape-level forest cover and distance to the nearest forest edge were equally unimportant for explaining understorey temperature offsets (Table S8).

Cross-validation of our models suggest that the GAMMs including canopy cover or canopy openness predict the offset of Tmax during summer reasonably well, with marginal R^2 values of 0.33 and 0.43, respectively (Appendix S11). These results further support the non-linear relationship between canopy cover and Tmax offset: the marginal R^2 value from the linear models (i.e. LMMs) including canopy cover was 0.24 and thus considerably lower than that of the GAMMs (0.33). However, the opposite was the case for canopy openness, with R^2 values of 0.43 and 0.24, respectively. SCA also had a moderate predictive performance, with a marginal R^2 value from cross-validated GAMM's of 0.20 for the offset of Tmax during summer. The predictive performances of basal area, crown area and tree height were low, with R^2 values ranging from 0.06 to 0.10 (Table S11).

Discussion

Understorey air temperature extremes in temperate lowland deciduous forests across Europe are considerably less severe than – or buffered from – those reported by weather stations outside forests, with mean (range) summer maximum and winter minimum ure offset values of -2.1 (-3.7 - 1.4) °C and 0.4 (-1.2 - 2.0) °C, respectively. Together with the spatial and temporal analysis of the drivers of the temperature offset, our results have important implications for improving the analysis of forest microclimates and their effects on forest biodiversity and functioning in the context of climate warming and land use change.

Canopy structure and composition play a key role in regulating the offset of maximum summer temperatures. Forests thus provide highly heterogeneous thermal environments, with maximum temperature conditions that are often much cooler than suggested by available climate layers (Scheffers *et al.*, 2017; Jucker *et al.*, 2018; Senior *et al.*, 2018). The maximum temperature offsets reported here compare well to general patterns observed in temperate regions across the globe and may even increase if the forest temperatures would be measured closer to the forest ground surface (De Frenne *et al.*, 2019). Local maximum temperatures greatly matter for the response of organisms to climate warming, because the relative fitness of a species is strongly related to the species-specific heat tolerance (Huey *et al.*, 2012). Many species living below tree canopies may therefore find thermal refuges within their habitats, allowing them to evade short-term temperature extremes (Scheffers *et al.*, 2014). Topographic microclimate heterogeneity and the associated provision of microrefugia reduces the climate-change-related extinction risk of plants and insects (Suggitt *et al.*, 2018) and our microclimate results suggest that this may also apply in forests; data on organismal responses are needed to explore this issue further. The future provision of thermal refuges will depend on the degree to which microclimates are decoupled from the macroclimate, potentially resulting in different warming rates under the canopy versus in the open (De Frenne *et al.*, 2019).

Changes in canopy structure and composition may alter local minimum and maximum temperatures at magnitudes exceeding the rates of macroclimate warming in the decades to come (IPCC, 2013). Habitat modifications resulting from a decrease of canopy cover, e.g. tree harvest in production forests, thus strongly intensify the local impact of macroclimate warming (and, conversely, increasing cover mitigates impact), which has significant implications for forest biodiversity dynamics and functioning. Habitat modifications in favour of warmer habitats matter for the re-assembly of terrestrial communities because the heat tolerance varies among species, putting species with low heat tolerances at higher risk of being filtered out (Nowakowski *et al.*, 2018). Incorporating canopy density information and associated shade effects into biophysical models of body temperatures is thus key to improve predictions of animals' vulnerability to climate change (Algar *et al.*, 2018). Increasing forest density, as has been observed in many temperate European forests as a consequence of changes in forest management over the past decades (e.g., Hedl *et al.*, 2010), may actually have compensated for, or even reversed, recent increases in maximum temperatures arising from anthropogenic global warming in some of these forests. Temperature buffering by trees also directly impacts human health and well-being, e.g. in cities, where trees alleviate human exposure to heat (Armson *et al.*, 2012). Considering the interactions between regional macroclimate warming and the local spatial and temporal dynamics in microclimates is thus crucial for the accurate assessment of the responses of forest biodiversity, ecosystem functioning and service provisioning to rapid global change.

The regulating effect of canopy structure and composition on understorey microclimate has long been embraced by forest ecologists and managers. Nevertheless, our finding that understory maximum temperatures are also regulated by differences in deciduous tree species composition, due to species-specific shade casting abilities, provides novel insights into the drivers of understory microclimates. We further show that the offset of maximum understorey

448 air temperatures is non-linearly related to canopy structure, e.g., to canopy cover, a proxy
449 variable for the understorey light conditions. Understorey temperature offsets may thus be
450 closely tied to the non-linear light absorption along the vertical canopy profile, as proposed by
451 the Beer-Lambert law (Monsi & Saeki, 1953). Together with findings from the tropics (Jucker
452 *et al.*, 2018) and temperate forests in Australia (Ashcroft & Gollan, 2012), who also found non-
453 linear effects of canopy cover on maximum temperatures, our results suggest that such non-
454 linear relationships may represent a general and globally relevant phenomenon, providing
455 important insights into the mechanisms governing forest microclimate gradients.

456 Forest managers and ecologists frequently use canopy structure *per se* (e.g. quantified
457 *via* variables such as canopy cover, basal area and LAI) as a proxy for understorey
458 microclimatic (including light) conditions, which are key drivers of forest regeneration and
459 species performance. Accounting for non-linear relationships between canopy structure, light
460 availability and extreme temperatures with associated threshold effects may help forest
461 managers to promote tree regeneration by creating or maintaining suitable tree species-specific
462 microclimatic conditions, or mitigate microclimate extremes and related damage to crops
463 produced in agroforestry schemes (Lin, 2007). In particular we found that canopy cover
464 increases daily absolute minimum temperatures during spring, confirming evidence that the
465 risks of spring frost damage on tree regeneration are reduced under canopy (Kollas *et al.*,
466 2013). Interpreting seasonal effects of canopy cover on microclimates would optimally be
467 based on data representing the seasonal variation in canopy cover, the lack of which being a
468 limitation to many studies, including ours. Investigating effects of temporal canopy cover
469 dynamics on microclimates thus provides an interesting avenue for further research. Moreover,
470 higher spring mean and maximum temperatures in forests compared to free-air conditions
471 may be driven by increased absorption of solar radiation by dark stems (bark) and remaining
472 leaf litter, resulting in accelerated snow melting and prolonged growing seasons (Wild *et al.*,
2014). Last but not

least, better knowledge about the relationship between canopy structure and microclimate will help to improve the ecological insights gained from investigations of forest structure-biodiversity relationships (Zellweger *et al.*, 2017), and will prove useful in attempts to maximise stepping stones and microrefugia in human dominated forest landscapes (Hannah *et al.*, 2014).

Understorey temperatures are regulated by complementing effects of local canopy attributes as well as topographic and landscape features derived at regional and landscape scales. Increasing daily and seasonal temperature ranges with increasing distance to the coast (continentality), result in higher offset values, e.g. owing to an increase in clear-sky days. Effects of microclimate buffering can thus be expected to be highest in dense forests in continental regions. Topographic position includes the effects of cold air drainage and pooling, which drive minimum temperatures during night and winter, particularly in calm, still conditions (Daly *et al.*, 2010; Dobrowski, 2011; Ashcroft & Gollan, 2012). Elevated locations inside forests may thus experience relatively warm temperatures, leading to longer snow-free periods and longer vegetation periods than suggested by macroclimate layers. Lower temperatures at topographic depressions enable persistent snow cover during winter, allowing winter-adapted plants and animals to overwinter in warmer and more stable conditions beneath the snow (Pauli *et al.*, 2013).

Our approach and analysis enable the approximation of forest temperatures based on widely available weather station data with high temporal resolution. While mechanistic downscaling of macroclimate data may achieve the same goal (Maclean *et al.*, 2018), our models can efficiently be used to predict understory temperatures form weather-station data, based on readily available that data about canopy structure and composition, as well as topography and landscape characteristics. For example, multitemporal canopy cover data collected within forest inventories can directly be used to make plot-level predictions of how

forest microclimates changed over time, and how this is related to responses of forest biodiversity and functioning to climate and land use change. Similarly, future scenarios of dynamics in canopy cover and composition can be incorporated into more realistic predictions of future forest climatic conditions and their ecological implications. Together with upcoming microclimate mapping techniques, such as the interpolation of *in situ* forest microclimate measurements using LiDAR remote sensing-based canopy cover maps (Zellweger *et al.*, 2019), the presented approach will be useful to fill the current gap of missing forest microclimate data (De Frenne & Verheyen, 2016).

Acknowledgements

FZ was funded by the Swiss National Science Foundation (grant no. 172198) and the Isaac Newton Trust. PDF received funding from the European Research Council (ERC) under the European Union's Horizon 2020 research and innovation programme (ERC Starting Grant FORMICA 757833). KV, LD and SLM received ERC funding through a Consolidator Grant (grant no. 614839: PASTFORWARD). DAC was funded by NERC (grant no. NE/K016377/1). MK was supported by the Czech Science Foundation (grant no. 17-13998S) and the Czech Academy of Sciences (grant no. RVO 67985939). FM was supported by project APVV-15-0270. We are grateful to all suppliers of weather station data, namely the Deutscher Wetterdienst (DWD), the Swedish Meteorological and Hydrological Institute (SMHI), the French meteorological institute (Météo France), Denise Pallett and the Upper Seeds automated weather station, and Zuzana Sitková and Katarína Střelcová, who were supported by projects APVV-16-0325 and VEGA 1/0367/16.

References

Algar, A.C., Morley, K. & Boyd, D.S. (2018) Remote sensing restores predictability of ectotherm body temperature in the world's forests. *Global Ecology and Biogeography*, **27**, 1412–1425.

Armson, D., Stringer, P. & Ennos, A.R. (2012) The effect of tree shade and grass on surface and globe temperatures in an urban area. *Urban Forestry & Urban Greening*, **11**, 245–255.

von Arx, G., Graf Pannatier, E., Thimonier, A., Rebetez, M. & Gilliam, F. (2013) Microclimate in forests with varying leaf area index and soil moisture: potential implications for seedling establishment in a changing climate. *Journal of Ecology*, **101**, 1201–1213.

Ashcroft, M.B. & Gollan, J.R. (2012) Fine-resolution (25 m) topoclimatic grids of near-surface (5 cm) extreme temperatures and humidities across various habitats in a large (200 × 300 km) and diverse region. *International Journal of Climatology*, **32**, 2134–2148.

Ashcroft, M.B. & Gollan, J.R. (2013) Moisture, thermal inertia, and the spatial distributions of near-surface soil and air temperatures: Understanding factors that promote microrefugia. *Agricultural and Forest Meteorology*, **176**, 77–89.

Barton, K. (2018) MuMIn: Multi-Model Inference. R package version 1.40.4.

Bates, D., Mächler, M., Bolker, B. & Walker, S. (2015) Fitting Linear Mixed-Effects Models using lme4. **67**.

Baudry, O., Charmetant, C., Collet, C. & Ponette, Q. (2014) Estimating light climate in forest with the convex densiometer : operator effect , geometry and relation to diffuse light. *European Journal of Forest Research*, **133**, 101–110.

Bazzaz, F.A. & Wayne, P.M. (1994) *Coping with environmental heterogeneity: the*

548 *physiological ecology of tree seedling regen- eration across the gap–understory*
549 *continuum*. *Exploitation of environmental heterogeneity by plants; ecophysiological*
550 *processes above and below ground* (ed. by M.M. Caldwell) and R.W. Pearcy), pp. 349–
551 390. Academic Press, New York.
552 Bivand, R. & Rundel, C. (2018) *rgeos: Interface to Geometry Engine - Open Source*
553 *('GEOS')*,.
554 Borcard, D., Legendre, P. & Drapeau, P. (1992) Partialling out the Spatial Component of
555 Ecological Variation. *Ecology*, **73**, 1045–1055.
556 Bramer, I., Anderson, B.J., Bennie, J., Bladon, A.J., De Frenne, P., Hemming, D., Hill, R.A.,
557 Kearney, M.R., Körner, C., Korstjens, A.H., Lenoir, J., Maclean, I.M.D., Marsh, C.D.,
558 Morecroft, M.D., Ohlemüller, R., Slater, H.D., Suggitt, A.J., Zellweger, F. &
559 Gillingham, P.K. (2018) Advances in Monitoring and Modelling Climate at Ecologically
560 Relevant Scales. *Advances in Ecological Research*, **58**, 101–161.
561 Chen, J., Saunders, S.C., Crow, T.R., Naiman, R.J., Brosofske, K.D., Mroz, G.D.,
562 Brookshire, B.L. & Franklin, J.F. (1999) Microclimate in forest ecosystem and
563 landscape ecology: Variations in local climate can be used to monitor and compare the
564 effects of different management regimes. *BioScience*, **49**, 288–297.
565 Daly, C., Conklin, D.R. & Unsworth, M.H. (2010) Local atmospheric decoupling in complex
566 topography alters climate change impacts. *International Journal of Climatology*, **30**,
567 1857–1864.
568 Davis, K.T., Dobrowski, S.Z., Holden, Z.A., Higuera, P.E. & Abatzoglou, J.T. (2019)
569 Microclimatic buffering in forests of the future: the role of local water balance.
570 *Ecography*, **42**, 1–11.
571 Dobrowski, S.Z. (2011) A climatic basis for microrefugia: the influence of terrain on climate.
572 *Global Change Biology*, **17**, 1022–1035.

EU-DEM (2018) EU-Digital Elevation Model (DEM).

FAO (2010) *Food and Agricultural Organization of the United Nations. Global Forest Resources Assessment 2010: Main Report. FAO Forestry Paper no. 163*,.

Fick, S.E. & Hijmans, R.J. (2017) WorldClim 2: new 1-km spatial resolution climate surfaces for global land areas. *International Journal of Climatology*, **37**.

De Frenne, P., Rodriguez-Sanchez, F., Coomes, D.A., Baeten, L., Verstraeten, G., Vellend, M., Bernhardt-Romermann, M., Brown, C.D., Brunet, J., Cornelis, J., Decocq, G.M., Dierschke, H., Eriksson, O., Gilliam, F.S., Hedl, R., Heinken, T., Hermy, M., Hommel, P., Jenkins, M.A., Kelly, D.L., Kirby, K.J., Mitchell, F.J., Naaf, T., Newman, M., Peterken, G., Petrik, P., Schultz, J., Sonnier, G., Van Calster, H., Waller, D.M., Walther, G.R., White, P.S., Woods, K.D., Wulf, M., Graae, B.J. & Verheyen, K. (2013) Microclimate moderates plant responses to macroclimate warming. *Proceedings of the National Academy of Sciences*, **110**, 18561–18565.

De Frenne, P. & Verheyen, K. (2016) Weather stations lack forest data. *Science*, **351**, 234.

De Frenne, P., Zellweger, F., Rodríguez-Sánchez, F., Scheffers, B., Hylander, K., Luoto, M., Vellend, M., Verheyen, K. & Lenoir, J. (2019) Global buffering of temperatures under forest canopies. *Nature Ecology & Evolution*.

Geiger, R., Aron, R.H. & Todhunter, P. (2003) *The climate near the ground*, Rowman and Littlefield, Oxford.

Greiser, C., Meineri, E., Luoto, M., Ehrlén, J. & Hylander, K. (2018) Monthly microclimate models in a managed boreal forest landscape. *Agricultural and Forest Meteorology*, **250**–**251**, 147–158.

Hannah, L., Flint, L., Syphard, A.D., Moritz, M.A., Buckley, L.B. & McCullough, I.M. (2014) Fine-grain modeling of species' response to climate change: holdouts, stepping-stones, and microrefugia. *Trends in Ecolgy and Evolution*, **29**, 390–397.

598 Hansen, M.C., Potapov, P. V, Moore, R., Hancher, M., Turubanova, S.A., Tyukavina, A.,
599 Thau, D., Stehman, S. V, Goetz, S.J., Loveland, T.R., Kommareddy, A., Egorov, A.,
600 Chini, L., Justice, C.O. & Townshend, J.R.G. (2013) High-Resolution Global Maps of
601 21st-Century Forest Cover Change. *Science*, **342**, 850–853.
602 Hedl, R., Kopecky, M. & Koma, J. (2010) Half a century of succession in a temperate
603 oakwood: from species-rich community to mesic forest. **16**, 267–276.
604 Hijmans, R.J. (2017) *raster: Geographic Data Analysis and Modeling*,.
605 Huey, R.B., Kearney, M.R., Krockenberger, A., Holtum, J.A., Jess, M. & Williams, S.E.
606 (2012) Predicting organismal vulnerability to climate warming: roles of behaviour,
607 physiology and adaptation. *Philos Trans R Soc Lond B Biol Sci*, **367**, 1665–1679.
608 IPCC (2013) *Climate change 2013: The Physical Science Basis. Contribution of Working*
609 *Group I to the Fifth Assessment Report of the Intergovern- mental Panel on Climate*
610 *Change*, Cambridge University Press, Cambridge, United Kingdom and New York, NY,
611 USA.
612 Jucker, T., Caspersen, J., Chave, J., Antin, C., Barbier, N., Bongers, F., Dalponte, M., van
613 Ewijk, K.Y., Forrester, D.I., Haeni, M., Higgins, S.I., Holdaway, R.J., Iida, Y., Lorimer,
614 C., Marshall, P.L., Momo, S., Moncrieff, G.R., Ploton, P., Poorter, L., Rahman, K.A.,
615 Schlund, M., Sonke, B., Sterck, F.J., Trugman, A.T., Usoltsev, V.A., Vanderwel, M.C.,
616 Waldner, P., Wedeux, B.M., Wirth, C., Woll, H., Woods, M., Xiang, W., Zimmermann,
617 N.E. & Coomes, D.A. (2016) Allometric equations for integrating remote sensing
618 imagery into forest monitoring programmes. *Global Change Biology*.
619 Jucker, T., Hardwick, S.R., Both, S., Elias, D.M.O., Ewers, R.M., Milodowski, D.T.,
620 Swinfield, T. & Coomes, D.A. (2018) Canopy structure and topography jointly constrain
621 the microclimate of human-modified tropical landscapes. *Global Change Biology*, **24**,
622 5243–5258.

623 Karger, D.N., Conrad, O., Böhner, J., Kawohl, T., Kreft, H., Soria-Auza, R.W.,
624 Zimmermann, N.E., Linder, H.P. & Kessler, M. (2017) Climatologies at high resolution
625 for the earth's land surface areas. *Scientific Data*, **4**, 170122.
626 Kearney, M.R. & Porter, W.P. (2017) NicheMapR – an R package for biophysical modelling:
627 the microclimate model. *Ecography*, **40**, 664–674.
628 Kollas, C., Körner, C. & Randin, C.F. (2013) Spring frost and growing season length co-
629 control the cold range limits of broad-leaved trees. *Journal of Biogeography*, **41**, 773–
630 783.
631 Kollas, C., Randin, C.F., Vitasse, Y. & Körner, C. (2014) How accurately can minimum
632 temperatures at the cold limits of tree species be extrapolated from weather station data?
633 *Agricultural and Forest Meteorology*, **184**, 257–266.
634 Kovács, B., Tinya, F. & Ódor, P. (2017) Stand structural drivers of microclimate in mature
635 temperate mixed forests. *Agricultural and Forest Meteorology*, **234**–**235**, 11–21.
636 Latimer, C.E. & Zuckerberg, B. (2017) Forest fragmentation alters winter microclimates and
637 microrefugia in human-modified landscapes. *Ecography*, **40**, 158–170.
638 Lenoir, J., Hattab, T. & Pierre, G. (2017) Climatic microrefugia under anthropogenic climate
639 change: implications for species redistribution. *Ecography*, **40**, 253–266.
640 Lin, B.B. (2007) Agroforestry management as an adaptive strategy against potential
641 microclimate extremes in coffee agriculture. *Agricultural and Forest Meteorology*, **144**,
642 85–94.
643 Maclean, I.M.D., Mosedale, J.R. & Bennie, J.J. (2018) Microclima: an R package for
644 modelling meso- and microclimate. *Methods in Ecology and Evolution*, **0**.
645 MEA (2005) *Millennium Ecosystem Assessment. Ecosystems and Human Well-being:*
646 *Biodiversity Sysnthesis*, World Resource Institute, Washington, DC.
647 Monsi, M. & Saeki, T. (1953) Uber den Lichtfaktor in den Pflanzengesellschaften und seine

Bedeutung fur die Stoffproduktion. *Japanese Journal of Botany*, **14**, 22–52.

Muggeo, V.M.R. (2017) Regression Models with Break-Points / Change-Points Estimation v. 0.5-3.0.

Nakagawa, S. & Schielzeth, H. (2012) A general and simple method for obtaining R2 from generalized linear mixed-effects models. *Methods in Ecology and Evolution*, **4**, 133–142.

Nowakowski, A.J., Watling, J.I., Thompson, M.E., Brusch, G.A. th, Catenazzi, A., Whitfield, S.M., Kurz, D.J., Suarez-Mayorga, A., Aponte-Gutierrez, A., Donnelly, M.A. & Todd, B.D. (2018) Thermal biology mediates responses of amphibians and reptiles to habitat modification. *Ecol Lett*, **21**, 345–355.

Pauli, J.N., Zuckerberg, B., Whiteman, J.P. & Porter, W. (2013) The subnivium: A deteriorating seasonal refugium. *Frontiers in Ecology and the Environment*, **11**, 260–267.

Potter, K.A., Arthur Woods, H. & Pincebourde, S. (2013) Microclimatic challenges in global change biology. *Global Change Biology*, **19**, 2932–2939.

R Core Team (2018) *R: A language and environment for statistical computing*, R Foundation for Statistical Computing, Vienna, Austria.

Renaud, V. & Rebetez, M. (2009) Comparison between open-site and below-canopy climatic conditions in Switzerland during the exceptionally hot summer of 2003. *Agricultural and Forest Meteorology*, **149**, 873–880.

Roberts, D.R., Bahn, V., Ciuti, S., Boyce, M.S., Elith, J., Guillera-Arroita, G., Hauenstein, S., Lahoz-Monfort, J.J., Schröder, B., Thuiller, W., Warton, D.I., Wintle, B.A., Hartig, F. & Dormann, C.F. (2017) Cross-validation strategies for data with temporal, spatial, hierarchical, or phylogenetic structure. *Ecography*, **40**, 913–929.

Rolland, C. (2003) Spatial and Seasonal Variations of Air Temperature Lapse Rates in Alpine

673 Regions. *Journal of Climate*, **16**, 1032–1046.
674 Scheffers, B.R., Edwards, D.P., Diesmos, A., Williams, S.E. & Evans, T.A. (2014)
675 Microhabitats reduce animal's exposure to climate extremes. *Global Change Biology*,
676 **20**, 495–503.
677 Scheffers, B.R., Edwards, D.P., Macdonald, S.L., Senior, R.A., Andriamahohatra, L.R.,
678 Roslan, N., Rogers, A.M., Haugaasen, T., Wright, P. & Williams, S.E. (2017) Extreme
679 thermal heterogeneity in structurally complex tropical rain forests. *Biotropica*, **49**, 35–
680 44.
681 Senior, R.A., Hill, J.K., Benedick, S. & Edwards, D.P. (2018) Tropical forests are thermally
682 buffered despite intensive selective logging. *Global Change Biology*, **24**, 1267–1278.
683 Suggitt, A.J., Wilson, R.J., Isaac, N.J.B., Beale, C.M., Auffret, A.G., August, T., Bennie, J.J.,
684 Crick, H.Q.P., Duffield, S., Fox, R., Hopkins, J.J., Macgregor, N.A., Morecroft, M.D.,
685 Walker, K.J. & Maclean, I.M.D. (2018) Extinction risk from climate change is reduced
686 by microclimatic buffering. *Nature Climate Change*, **8**, 713–717.
687 Uvarov, B.P. (1931) Insects and climate. *Transactions of the Royal Entomological Society of*
688 *London*, **79**, 1–232.
689 Verheyen, K., Baeten, L., De Frenne, P., Bernhardt-Römermann, M., Brunet, J., Cornelis, J.,
690 Decocq, G., Dierschke, H., Eriksson, O., Hédl, R., Heinken, T., Hermy, M., Hommel,
691 P., Kirby, K., Naaf, T., Peterken, G., Petřík, P., Pfadenhauer, J., Van Calster, H.,
692 Walther, G.-R., Wulf, M. & Verstraeten, G. (2012) Driving factors behind the
693 eutrophication signal in understorey plant communities of deciduous temperate forests.
694 *Journal of Ecology*, **100**, 352–365.
695 Wild, J., Kopeck, M., Svoboda, M., Zenahlikova, J., Edwards-Jonasova, M. & Herben, T.
696 (2014) Spatial patterns with memory : tree regeneration after stand-replacing disturbance
697 in Picea abies mountain forests. **25**, 1327–1340.

Wood, S.N. (2017) *Generalized Additive Models: An Introduction with R*, 2nd edn. Chapman and Hall/CRC.

Zellweger, F., Frenne, P. De, Lenoir, J., Rocchini, D. & Coomes, D. (2019) Advances in microclimate ecology arising from remote sensing. *Trends in Ecology & Evolution*.

Zellweger, F., Roth, T., Bugmann, H. & Bollmann, K. (2017) Beta diversity of plants, birds and butterflies is closely associated with climate and habitat structure. *Global Ecology and Biogeography*, **26**, 898–906.

Zuur, A.F., Ieno, E.N., Walker, N.J., Saveliev, A.A. & Smith, G.M. (2009) *Mixed Effects Models and Extensions in Ecology with R*, Springer, New York.

Biosketch

We are broadly interested in the responses of forest biodiversity and functioning to climate and land-use change. We are particularly interested in the role of forest microclimate dynamics in driving these responses.

Data Accessibility Statement

Data will be uploaded to a Pangaea database.

Table 1. Overview and summary statistics of predictor variables used to explain understorey temperature offsets. Northness, slope, elevation and topographic position were derived from EU-DEM (2018). Note that high values of basal area and crown area derive from inclusion of some large trees at the edge of the plots.

Variable group	Variable name	Description	Range (mean)	Unit
Local canopy structure and composition				
	Canopy cover	Visual estimation of vertical cover of shrub and tree layers, summed per species	41 – 213 (112)	%
	Canopy openness	Total number of quadrats of open sky visible on spherical densiometer	3.9 – 59.50 (15.7)	Number
	Basal area	Basal area of trees with DBH > 7.5 cm	5.2 – 122.3 (33.2)	m^2/ha
	Crown area	Predicted crown area per plot based on scaling relationships with DBH (Jucker *et al.*, 2016)	53.4 – 1199 (309.1)	m^2
	Tree height	Height of tree on which temperature sensor was placed; measured using a vertex hypsometer (Vertex IV)	9.2 – 40.0 (26.2)	m
	Shade casting ability	Tree-species-specific shade casting ability based on (Verheyen *et al.*, 2012), community-level mean index weighted by tree species-specific canopy cover.	2.1 – 5 (3.6)	1 (tree species with very open canopy) to 5 (very dense & shady species)
Landscape structure and topography				
	Forest cover	Proportion of area covered by forest within a circular buffer area with a radius of 250m (Hansen *et al.*, 2013)	18.1 – 100.0 (96.3)	%
	Distance to forest edge	Distance to nearest forest edge (Hansen *et al.*, 2013)	1.0 – 728.3 (119)	m
	Northness	Cosine of topographic aspect. Northness is a continuous variable describing the topographic exposition ranging from completely north exposed (-1) to completely south exposed (1).	-1.0 – 1.0 (-0.3)	index
	Slope	Topographic slope	0.4 – 22.0 (4.3)	Degrees
	Elevation	Elevation above sea level	30.7 – 636.9 (165.7)	m
	Topographic position	Relative topographic position describing the plot elevation in relation to the surrounding elevations. Valley bottoms have low values, elevated locations, such as ridges, have high values	1.6 – 147.3 (23.5)	m
	Distance to coast	Distance to nearest coastline derived from Natural Earth (free vector and raster map data from naturalearthdata.com)	11.6 – 518.7 (107.6)	km

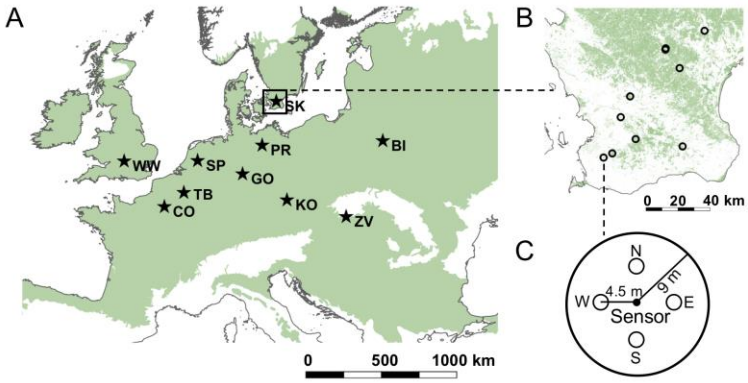

Figure 1. Sampling design showing (a) the distribution of the ten sampled regions across the temperate deciduous forest biome in Europe (green area); (b) an example region (SK) and its forest cover taken from Hansen *et al.* (2013), with ten plots spread along the regional gradient of canopy cover; (c) the plot sampling design with the four interpretation points in each cardinal direction, as described in the main text. WW: Wytham, CO: Compiègne, TB: Tournibus, SP: Speulderbos, GO: Göttingen, PR: Prignitz, SK: Skane, KO: Koda, ZV: Zvolen, BI: Bialowieza.

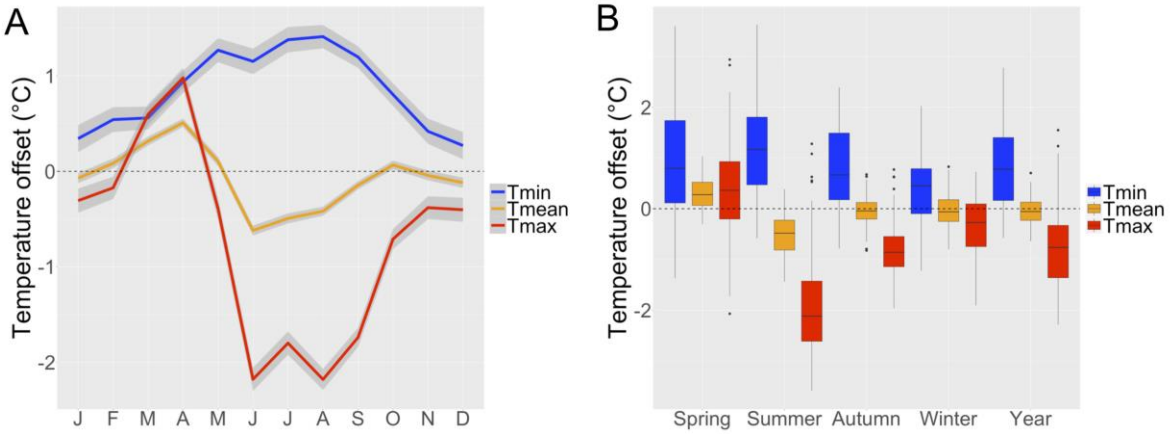

Figure 2. A: Daily air temperature offsets per month with 95 %-confidence intervals (grey ribbons), measured during one year in the understorey of temperate deciduous forests in Europe (Figure 1). B: Distributions of temperature offset values during spring (March to May), summer (June to August), autumn (September to November), winter (December to February), and the entire year. Positive values indicate warmer and negative values indicate cooler conditions in the understorey compared to nearby free-air conditions measured by weather stations.

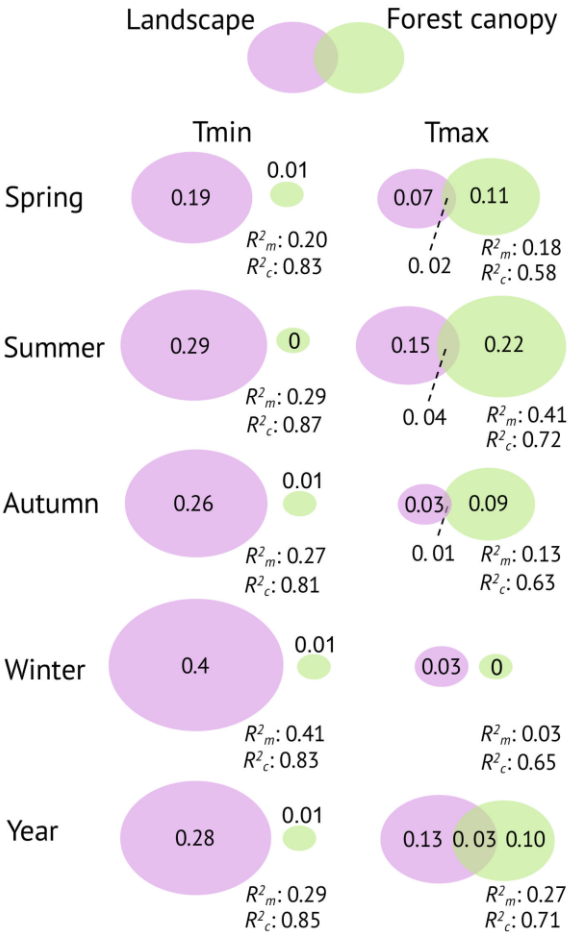

Figure 3. Venn-Euler diagrams showing the independent share of explained variation (R^2_m) for each variable group, i.e., landscape and forest canopy, as well as the shared amount of explained variation (intersection of ellipses), as determined by variation partitioning. The sizes of the ellipses are scaled according to R^2_m. Marginal R^2 (R^2m) describes variation explained by fixed factors only; conditional R^2 (R^2c) the variation explained by the fixed and random factors together.

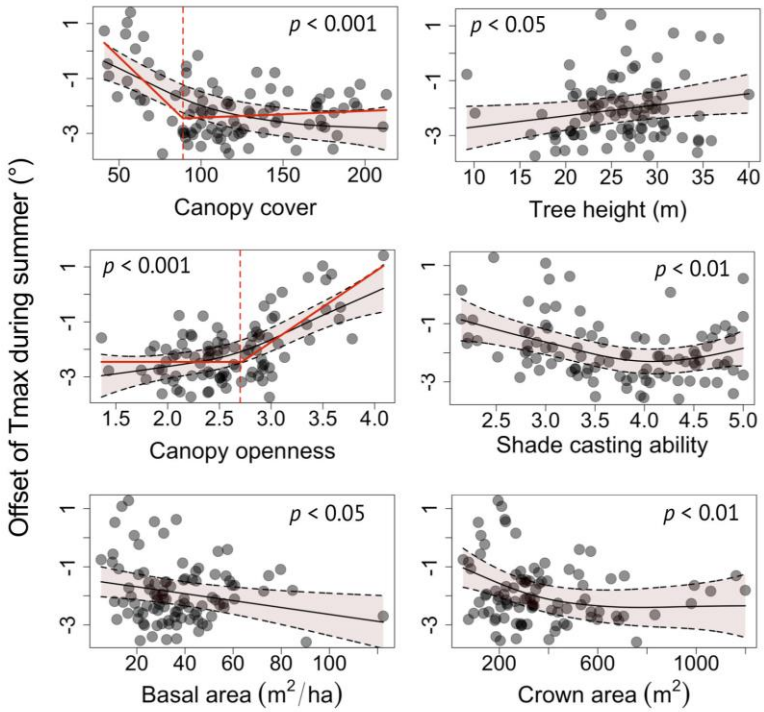

Figure 4. Relationships between canopy characteristics and the offset of daily maximum temperatures during summer. Smoothed curves with 95 % confidence intervals (light red polygons) and *p*-values from the GAMMs. Canopy openness was log-transformed. Canopy cover and canopy openness show non-linear relationships, with break points at 89 % and 2.7, respectively, as indicated by the red dashed lines. The solid red lines show the regression lines as calculated using piecewise regression (see text for details). We did not elaborate on threshold effects for shade casting ability and crown area because of large confidence intervals. Positive offset values represent warmer temperatures inside than outside forests, negative offset values indicate cooler temperatures inside than outside forests.

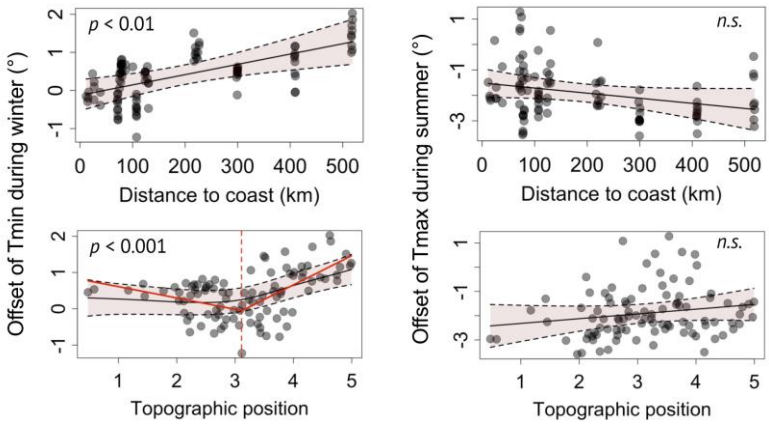

Figure 5. Relationships between the distance to coast and relative topographic position (log-transformed, low values representing valley bottoms; high values representing elevated locations, e.g. ridges) and the offset of daily minimum temperatures during winter, and daily maximum temperatures during summer. Topographic position was non-linearly related to Tmin offset during winter, with a threshold at 3.1 (standard error 0.16), as indicated by the red dashed line. 95 % confidence intervals (light red polygons) and *p*-values from the GAMMs are shown. Positive offset values represent warmer temperatures inside than outside forests, negative offset values indicate cooler temperatures inside than outside forests.